ISA Transactions 48 (2009) 148–155

Contents lists available at ScienceDirect

ISA Transactions

journal homepage: www.elsevier.com/locate/isatrans

On the design of fuzzified trajectory shaping guidance law

Chun-Liang Lin *, Yu-Ping Lin, Kai-Ming Chen

Department of Electrical Engineering, National Chung Hsing University, Taichung, 402, Taiwan, ROC

ARTICLE INFO

Article history:
Received 18 July 2008
Received in revised form
20 October 2008
Accepted 3 November 2008
Available online 2 December 2008

Keywords:
Missile
Guidance
Neuron fuzzy system
Trajectory shaping

ABSTRACT

Midcourse guidance is commonly designed to save as much energy as possible so that the missile's final speed can be maximized while entering the homing stage. For this purpose, a competitive guidance design should be able to generate an admissible flight trajectory as to bring the interceptor to a superior altitude for a favorable target engagement. In this paper, a new adaptive trajectory shaping guidance scheme based on the adaptive fuzzy inference system, which is capable of generating a variety of trajectories for efficient target interception, is presented. The guidance law is developed with the aim of saving the interceptor's energy conservation while improving performance robustness. Applications of the presented approach have included a variety of mission oriented guidance, such as cruise missile guidance, anti-ballistic missile guidance, etc.

1. Introduction

A multitude of guidance design techniques, such as linear quadratic regulator (LQR) [1] modified proportional guidance [2] and geometric control [3] have been proposed in the literature for implementation of the optimal midcourse or terminal guidance laws. In particular, LQR and neural networks have recently been applied to deal with the anti-ballistic missile guidance design problem [4]. Traditionally, midcourse guidance was formulated mostly as an optimal control problem to shape the flight trajectory and to maximize the terminal speed or minimize the flight time. However, solving LQR problems or training neural networks in real-time is often practically infeasible. Neural network guidance might be unreliable in practice if the neural network was not well trained. It is very common that neural network sensibly interpolates input data that are new to the network, causing unpredictable outputs. Fuzzy logic conceptually possesses the quality of robustness. It is well known that fuzzy systems have the ability to make use of knowledge in expressing in the form of linguistic rules without resorting to the precise model. However, its early application relied on trial and error while selecting either the membership functions or the fuzzy rules. An adaptive fuzzy logic controller working as an adaptive neural-fuzzy inference system (ANFIS) relieves this stringent requirement [5]. Some researchers also attempted to apply fuzzy logic theory to missile guidance designs [6–9].

Literature detailing the issues of modern guidance law design subjects to multi-boundary conditions is quite rare. A spline missile guidance law possesses a generalized interpolating structure that artificially allows reshaping the flight trajectory with respect to the specified via points and two boundary conditions. Although increasing attention has been devoted to the applications of fuzzy logic on missile guidance and control, the fuzzy spline guidance design has rarely been attempted. Here, the interceptor's flight trajectory is reshaped by combining ANFIS with spline guidance to navigate the missile's flight through the specified midpoints for lower control energy consumption and a favorable target engagement. Based on the adaptation feature, the guidance law is shown as to achieve better performance robustness than the guidance law, simply with constant navigation gains.

2. Generalized trajectory shaping guidance

Suppose that the inertial frame is located at the ground tracker. The present position, velocity, and midpoints of the interceptor are defined as

$$r(t_0) = (x_0, y_0, z_0), \qquad v(t_0) = (\dot{x}_0, \dot{y}_0, \dot{z}_0),$$
$$r_A(t_A) = (x_A, y_A, z_A), \qquad r_B(t_B) = (x_B, y_B, z_B)$$

where x is the downrange, y, the cross range, and z, the altitude; the subscripts 0, A, and B of t represent, respectively, the initial time, the time at midpoint A and the time at midpoint B. The acceleration command vector is to be determined:

$$a_c(t) = [a_x(t), a_y(t), a_z(t)], \quad t_0 \le t \le t_f$$

where t_f is the final flight time. Equations of motion of the interceptor in Cartesian coordinates are

$$\begin{aligned} \dot{x} &= v_x, & \dot{v}_x &= a_x, \\ \dot{y} &= v_y, & \dot{v}_y &= a_y, \\ \dot{z} &= v_z, & \dot{v}_z &= a_z + g \end{aligned} \tag{1}$$

* Corresponding author. Tel.: +886 4 22851549x708; fax: +886 4 22851410.
E-mail address: chunlin@dragon.nchu.edu.tw (C.-L. Lin).

0019-0578/$ – see front matter © 2008 ISA. Published by Elsevier Ltd. All rights reserved.
doi:10.1016/j.isatra.2008.11.001

where g is the gravity acceleration. For the target, let

$$\begin{aligned} \dot{x}_t &= -v_{tx}, \qquad \dot{v}_{tx} = a_{tx}, \\ \dot{y}_t &= -v_{ty}, \qquad \dot{v}_{ty} = a_{ty}, \\ \dot{z}_t &= -v_{tz}, \qquad \dot{v}_{tz} = a_{tz} + g \end{aligned} \tag{2}$$

where a_{tx}, a_{ty} and a_{tz} are disturbance inputs.

Define the relative range between the interceptor and the target as

$$R = \sqrt{R_{mtx}^2 + R_{mty}^2 + R_{mtz}^2}$$

where $R_{mtx} = x_t - x$, $R_{mty} = y_t - y$, and $R_{mth} = z_t - z$. The midpoints $r_A(t_A)$ and $r_B(t_B)$ are pre-specified, and the predicted interception point are given by

$$x_f = x_0 + v_x T_{go}, \qquad y_f = y_0 + v_y T_{go}, \qquad z_f = z_0 + v_z T_{go}$$

where $(x_f, y_f, z_f) = (x(t_f), y(t_f), z(t_f))$ and $T_{go} \approx R/v_c$ with v_c denoting the closing velocity between the interceptor and the target.

In previous research, the proportional navigation guidance law has been shown to be a special case of the explicit guidance law [10], while explicit guidance is a special case of spline guidance. The spline guidance law will be abbreviated as S–N guidance law according to the number of via points, which includes two boundary conditions and N-2 midpoints.

S–N guidance law considers the diagonal linear system of the form [11,12]:

$$\begin{bmatrix} 2\Delta t_1 & \Delta t_1 & & & 0 \\ \Delta t_1 & 2(\Delta t_1 + \Delta t_2) & \Delta t_1 & & \\ & \ddots & \ddots & \ddots & \\ & & \Delta t_{n-2} & 2(\Delta t_{n-2} + \Delta t_{n-1}) & \Delta t_{n-1} \\ 0 & & & \Delta t_{n-1} & 2\Delta t_{n-1} \end{bmatrix} \times \begin{bmatrix} \ddot{x}_0 \\ \ddot{x}_1 \\ \vdots \\ \ddot{x}_{n-2} \\ \ddot{x}_f \end{bmatrix} = 6 \begin{bmatrix} \Delta x_1/\Delta t_1 - \dot{x}_0 \\ \Delta x_2/\Delta t_2 - \Delta x_1/\Delta t_1 \\ \vdots \\ \Delta x_{n-1}/\Delta t_{n-1} - \Delta x_{n-2}/\Delta t_{n-2} \\ \dot{x}_f - \Delta x_{n-1}/\Delta t_{n-1} \end{bmatrix}$$

where $x_f = x_N$. The acceleration command can be rewritten as

$$\ddot{x}_c(t) = \ddot{x}_{k-1} P_1(t) + \ddot{x}_k P_2(t), \quad t_{k-1} \le t \le t_k, k = 1, 2, \ldots, N-1$$

where $P_1(t)$ and $P_2(t)$, the pre-specified functions of time, are linearly independent.

To simplify implementation, the following functions are chosen

$$P_1(t) = 1, \qquad P_2(t) \cong 0.$$

That is

$$\ddot{x}_c(t) = \ddot{x}_{k-1}, \quad k = 1, 2, \ldots, N-1.$$

One should be particularly interested in $N = 4$. For that case, the guidance law can be viewed as the generalization of S-4, S-3, and S-2 guidance laws. Fig. 1 shows three guidance phases of S-4 guidance law. During the first phase, the interceptor is guided by S-4 guidance law, the interceptor in the second phase is guided by S-3 guidance law, and the interceptor in the last phase is guided by S-2 guidance law. On the basis of this arrangement, it is possible to construct a variety of favorable flight trajectories to effectively intercept targets from various incoming directions. For example, one may set $x_A \le x_B < x_f$ to reach a near head-on interception for ballistic targets. By setting $x_A > x_B \approx x_f$, the interceptor could act to engage cruise targets. Fig. 2 displays three representative flight trajectories.

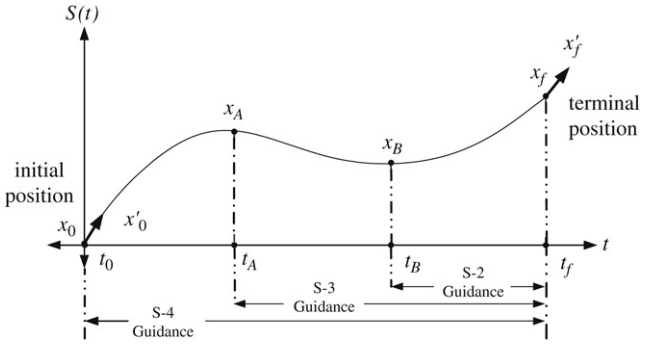

Fig. 1. S-4 guidance phases.

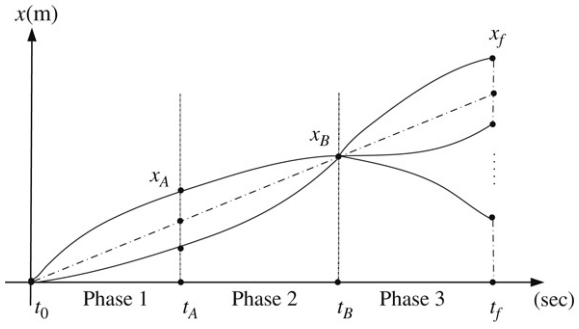

Fig. 2. Various trajectories generated by the S-4 guidance law.

2.1. Derivation of S-4 guidance law

Let the S-4 trajectory be denoted as $S(t)$, which passes through x_0, x_f, and two midpoints x_1, x_2. Define a three-order polynomial f_k as follows

$$f_k(t) = A_k(t - t_{k-1})^3 + B_k(t - t_{k-1})^2 + C_k(t - t_{k-1}) + D_k, \quad k = 1, 2, 3 \tag{3}$$

where A_k, B_k, C_k and D_k, $k = 1, 2, 3$, are coefficients to be determined. $S(t)$ has to satisfy two boundary conditions with velocity and the positions of two midpoints.

The conditions for the continuity of the splines at the knots are given by

(i)

$$\begin{aligned} x_{k-1} &= f_k(t_{k-1}) = D_k, \\ x_k &= f_k(t_k) = A_k \Delta t_k^3 + B_k \Delta t_k^2 + C_k \Delta t_k + D_k \end{aligned} \tag{4}$$

(ii)

$$\begin{aligned} \dot{x}_{k-1} &= \dot{f}_k(t_{k-1}) = C_k, \\ \dot{x}_k &= \dot{f}_k(t_k) = 3A_k \Delta t_k^2 + 2B_k \Delta t_k + C_k \end{aligned} \tag{5}$$

(iii)

$$\begin{aligned} \ddot{x}_{k-1} &= \ddot{f}_k(t_{k-1}) = 2B_k, \\ \ddot{x}_k &= \ddot{f}_k(t_k) = 6A_k \Delta t_k + 2B_k \end{aligned} \tag{6}$$

where $\Delta t_k = t_k - t_{k-1}$. From (4) and (6), one gets

$$\begin{aligned} A_k &= \frac{1}{6\Delta t_k}(\ddot{x}_k - \ddot{x}_{k-1}), \qquad B_k = \frac{1}{2}\ddot{x}_{k-1}, \\ C_k &= \frac{\Delta x_k}{\Delta t_k} - \frac{\Delta t_k}{6}(\ddot{x}_k + 2\ddot{x}_{k-1}), \qquad D_k = x_{k-1} \end{aligned} \tag{7}$$

where $\Delta x_k = x_k - x_{k-1}$.

Substituting (7) into (5), one further obtains

$$x_{k-1} = \frac{\Delta x_k}{\Delta t_k} - \frac{1}{6}\Delta t_k(\ddot{x}_k + 2x_{k-1}), \quad k = 1, 2, 3 \tag{8}$$

and

$$\dot{x}_k = \frac{\Delta x_k}{\Delta t_k} + \frac{1}{6}\Delta t_k(2\ddot{x}_k + 2x_{k-1}). \tag{9}$$

Differentiation of $S(t)$ should be continuous at the knots, i.e.

$$\dot{f}_{k-1}(t_{k-1}) = \dot{f}_k(t_{k-1}), \quad k = 2, 3. \tag{10}$$

By substituting (5) into (10), one obtains the following recursive equations:

$$3A_{k-1}\Delta t_{k-1}^2 + 2B_{k-1}\Delta t_{k-1} + C_{k-1} = C_k, \quad k = 2, 3. \tag{11}$$

Substituting (7) into (10), gives

$$\begin{aligned}&\Delta t_{k-1}\ddot{x}_{k-2} + 2(\Delta t_{k-1} + \Delta t_k)\ddot{x}_{k-1} + \Delta t_k\ddot{x}_k \\ &\quad = 6\left(\frac{\Delta x_k}{\Delta t_k} - \frac{\Delta x_{k-1}}{\Delta t_{k-1}}\right), \quad k = 2, 3.\end{aligned} \tag{12}$$

There are two equations and four unknown acceleration terms. Therefore, two extra conditions should be available. From (8) and (9), one has

$$2\Delta t_1\ddot{x}_0 + \Delta t_1\ddot{x}_1 = 6\left(\frac{\Delta x_1}{\Delta t_1} - \ddot{x}_0\right), \tag{13}$$

$$\Delta t_3\ddot{x}_2 + 2\Delta t_3\ddot{x}_3 = 6\left(\dot{x}_3 - \frac{\Delta x_3}{\Delta t_3}\right). \tag{14}$$

Eqs. (12)–(14) now constitute a tri-diagonal linear system of equations. From which one can have $\ddot{x}_i$, $i = 1, \ldots, 4$, determined by

$$\begin{bmatrix}\ddot{x}_0\\ \ddot{x}_1\\ \ddot{x}_2\\ \ddot{x}_3\end{bmatrix} = \frac{2}{\eta\Delta t_2}\begin{bmatrix}2\eta_1 & -\eta_2 & 2 & -1\\ -\eta_2 & 2\eta_2 & -4 & 2\\ 2 & -4 & 2\eta_3 & -\eta_3\\ -1 & 2 & -\eta_3 & 2\eta_4\end{bmatrix}\begin{bmatrix}\alpha_1\\ \alpha_2\\ \alpha_3\\ \alpha_4\end{bmatrix}$$

where $\alpha_1 = \Delta x_1/\Delta t_1 - \dot{x}_0$, $\alpha_2 = \Delta x_2/\Delta t_2 - \Delta x_1/\Delta t_1$, $\alpha_3 = \Delta x_3/\Delta t_3 - \Delta x_2/\Delta t_2$, $\alpha_4 = \dot{x}_f - \Delta x_3/\Delta t_3$; $\eta = 4(1+\Delta t_1/\Delta t_2)(1+\Delta t_3/\Delta t_2) - (\Delta t_1/\Delta t_2)(\Delta t_3/\Delta t_2)$, $\eta_1 = 3(1 + \Delta t_2/\Delta t_1)(1 + \Delta t_3/\Delta t_2) + 1$, $\eta_2 = 3(1+\Delta t_3/\Delta t_2) + 1$, $\eta_3 = 3(1+\Delta t_1/\Delta t_2) + 1$, $\eta_4 = 3(1 + \Delta t_1/\Delta t_2)(1 + \Delta t_2/\Delta t_3) + 1$; $\Delta t_1 = t_A - t_0$, $\Delta x_1 = x_1 - x_0$, $\Delta t_2 = t_B - t_A$, $\Delta x_2 = x_2 - x_1$, $\Delta t_3 = t_f - t_B$, $\Delta x_3 = x_f - x_2$.

For briefness, define $T_{go} = \Delta t_1 + \Delta t_2 + \Delta t_3$, $T_{goB} = \Delta t_1 + \Delta t_2$ and $T_{goA} = \Delta t_1$. S-4 guidance law is determined via the following equations:

$$\ddot{x}_c(t) = \ddot{x}_{k-1}, \quad t_{k-1} < t \le t_k, k = 1, 2, 3. \tag{15}$$

Phase 1: $(t_0 < t \le t_A)$

The primary objective of this phase is to guide the interceptor to an appropriate altitude and to avoid excessive energy loss while achieving a higher speed.

The guidance command during this phase is derived as

$$\begin{aligned}\ddot{x}_0 &= \frac{2}{\eta\Delta t_2}(2\eta_1\alpha_1 - \eta_2\alpha_2 + 2\alpha_3 - \alpha_4)\\ &= \frac{2}{4T_{go} + 3\frac{\Delta t_1\Delta t_3}{\Delta t_2}}\left[6\chi\frac{\Delta x_1}{\Delta t_1} - 6\chi\dot{x}_0 - 3\frac{\Delta t_3}{\Delta t_2}\frac{\Delta x_2}{\Delta t_2} + 3\frac{\Delta t_3}{\Delta t_2}\frac{\Delta x_1}{\Delta t_1}\right.\\ &\quad \left. + 12\frac{\Delta x_1}{\Delta t_1} - 6\frac{\Delta x_2}{\Delta t_2} + 3\frac{\Delta x_3}{\Delta t_3} - 8\dot{x}_0 - \dot{x}_f\right]\end{aligned}$$

where $\chi = \frac{\Delta t_3}{\Delta t_2} + \frac{\Delta t_2}{\Delta t_1} + \frac{\Delta t_3}{\Delta t_1}$. Clearly, when $\Delta t_1 \approx \Delta t_2 \approx \Delta t_3$, it can be simplified as

$$\begin{aligned}\ddot{x}_0 = \frac{2}{5}\Bigg[&-\frac{(\dot{x}_f - \dot{x}_0)}{T_{go}} - \frac{6(\Delta x_2/\Delta t_2 - \Delta x_1/\Delta t_1)}{T_{go}}\\ &+ \frac{3(\Delta x_3/\Delta t_3 - \Delta x_2/\Delta t_2)}{T_{go}} + \frac{9(x_1 - x_0 - \dot{x}_0 T_{goA})}{T_{goA}^2}\Bigg]\end{aligned} \tag{16}$$

where $\Delta x_2/\Delta t_2 - \Delta x_1/\Delta t_1$ and $\Delta x_3/\Delta t_3 - \Delta x_2/\Delta t_2$ are, respectively, the curvature changes of phases 1 and 2; $x_1 - x_0 - \dot{x}_0 T_{goA}$ is the position error at point A.

Phase 2: $(t_A < t \le t_B)$

The objective is to shape an appropriate flight trajectory so that the guidance commands generated in Phase 1 would be smoothly transferred to the next guidance phase.

The acceleration command during the period $[t_A, t_B]$ is given by

$$\ddot{x}_1 = \frac{2}{\eta\Delta t_2}(-\eta_2\alpha_1 + 2\eta_2\alpha_2 - 4\alpha_3 + 2\alpha_4).$$

As $T_{goA} \to 0$, the interceptor arrives at midpoint A, we get $\lim_{\Delta t_1 \to 0}\Delta x_1/\Delta t_1 = \dot{x}_0$ and $\alpha_1 \to 0$, then

$$\begin{aligned}\ddot{x}_1 = &\frac{\dot{x}_f - \dot{x}_0}{T_{go}} - \frac{3(\Delta x_3/\Delta t_3 - \Delta x_2\Delta t_3/\Delta t_2^2)}{T_{go}}\\ &+ \frac{6(x_2 - x_0 - \dot{x}_0\Delta t_2)}{(\Delta t_2 + \Delta t_3)\Delta t_2}.\end{aligned}$$

When $\Delta t_1 \approx \Delta t_2 \approx \Delta t_3$, $\ddot{x}_1$ reduces to

$$\begin{aligned}\ddot{x}_1 = &\frac{\dot{x}_f - \dot{x}_0}{T_{go}} - \frac{3(\Delta x_3/\Delta t_3 - \Delta x_2/\Delta t_2)}{T_{go}}\\ &+ \frac{3(x_2 - x_0 - \dot{x}_0 T_{goB})}{T_{goB}^2}\end{aligned} \tag{17}$$

where $\Delta t_2 = T_{goB} - T_{goA}$ and $T_{goA} = 0$ when $t_A < t \le t_B$. When $x_0 = x_A$, S-4 guidance reduces to S-3 guidance.

Phase 3: $(t_B < t \le t_f)$

Since the position error dominates the final missile distance, the major objective during this phase is to fully develop the missile's terminal engagement performance. The navigation term contributed by the position error should contribute to effective acceleration command so that the accumulated tracking errors can be significantly reduced.

The acceleration command in the period $(t_B, t_f]$ is given by

$$\ddot{x}_2 = \frac{2}{\eta\Delta t_2}(2\alpha_1 - 4\alpha_2 + 2\eta_3\alpha_3 - \eta_3\alpha_4).$$

As $T_{goB} \to 0$, the interceptor passes through point B, then $\lim_{\Delta t_2 \to 0}\Delta x_2/\Delta t_2 = \dot{x}_0$, $\alpha_1 = \alpha_2 \to 0$, $\Delta t_3 = T_{go}$ and

$$\begin{aligned}\ddot{x}_2 = \frac{2}{4T_{go} + 3\frac{\Delta t_1\Delta t_3}{\Delta t_2}}\Bigg\{&-\left[\left(4 + 3\frac{\Delta t_1}{\Delta t_2}\right)\dot{x}_f - 7\dot{x}_0\right]\\ &- \left(15 + 6\frac{\Delta t_1}{\Delta t_2}\right)\dot{x}_0 + \left(9\frac{\Delta t_1}{\Delta t_2} + 12\right)\frac{\Delta x_3}{\Delta t_3}\Bigg\}.\end{aligned}$$

It can be seen easily that as $\Delta t_1 \to 0$ and $\Delta t_2 \to 0$, i.e. x_A is close to x_B, then S-3 guidance law becomes the known explicit guidance law [10]:

$$\ddot{x}_2 = \frac{-2(\dot{x}_f - \dot{x}_0)}{T_{go}} + \frac{6(x_f - x_0 - \dot{x}_0 T_{go})}{T_{go}^2}. \tag{18}$$

Under the assumptions of $\Delta t_1 \approx \Delta t_2 \approx \Delta t_3$, the acceleration commands in the inertial frame can be summarized as follows

$$\begin{aligned}
\ddot{x}_0 &= \frac{2}{5}\left[-\frac{(\dot{x}_f-\dot{x}_0)}{T_{go}} - \frac{6(\Delta x_2/\Delta t_2 - \Delta x_1/\Delta t_1)}{T_{go}} \right. \\
&\quad \left. + \frac{3(\Delta x_3/\Delta t_3 - \Delta x_2/\Delta t_2)}{T_{go}} + \frac{9(x_1 - x_0 - \dot{x}_0 T_{goA})}{T_{goA}^2} \right], \\
&\quad t_0 \le t \le t_A \\
\ddot{x}_1 &= \frac{(\dot{x}_f-\dot{x}_0)}{T_{go}} - \frac{3(\Delta x_3/\Delta t_3 - \Delta x_2/\Delta t_2)}{T_{go}} \\
&\quad + \frac{3(x_2 - x_0 - \dot{x}_0 T_{goB})}{T_{goB}^2}, \quad t_A < t \le t_B \\
\ddot{x}_2 &= \frac{-2(\dot{x}_f-\dot{x}_0)}{T_{go}} + \frac{6(x_f - x_0 - \dot{x}_0 T_{go})}{T_{go}^2}, \quad t_B < t \le t_f.
\end{aligned} \tag{19}$$

The guidance commands for the Y-axis can be obtained analogously. And, the guidance commands for the Z-axis are

$$\begin{aligned}
\ddot{z}_0 &= \frac{2}{5}\left[-\frac{(\dot{z}_f-\dot{z}_0)}{T_{go}} - \frac{6(\Delta z_2/\Delta t_2 - \Delta z_1/\Delta t_1)}{T_{go}} \right. \\
&\quad \left. + \frac{3(\Delta z_3/\Delta t_3 - \Delta z_2/\Delta t_2)}{T_{go}} + \frac{9(z_1 - z_0 - \dot{z}_0 T_{goA})}{T_{goA}^2} \right] + g, \\
&\quad t_0 \le t \le t_A \\
\ddot{z}_1 &= \frac{(\dot{z}_f-\dot{z}_0)}{T_{go}} - \frac{3(\Delta z_3/\Delta t_3 - \Delta z_2/\Delta t_2)}{T_{go}} \\
&\quad + \frac{3(z_2 - z_0 - \dot{z}_0 T_{goB})}{T_{goB}^2} + g, \quad t_A < t \le t_B \\
\ddot{z}_2 &= \frac{-2(\dot{z}_f-\dot{z}_0)}{T_{go}} + \frac{6(z_f - z_0 - \dot{z}_0 T_{go})}{T_{go}^2} + g, \quad t_B < t \le t_f.
\end{aligned} \tag{20}$$

It should be noted that, after some transformations, the command switching can be altered to the relative range between the interceptor and the target.

In the trajectory shaping guidance scheme developed above, the acceleration command with constant gains are adequate for a target engagement when the relative range between the interceptor and the target is relatively short. However, it is highly desirable to further improve its performance robustness since the guidance law with constant gains is robust enough to withstand environmental changes and target maneuvers. This gives rise to the requirement of the functionally adaptive feature.

3. Adaptive S-4 guidance law

The guidance parameters of the S-guidance law become dynamically tunable by introducing the architecture of ANFIS. ANFIS is a class of adaptive networks that are functionally equivalent to fuzzy inference systems. ANFIS represents both the Sugeno and Tsukamoto fuzzy models and use a hybrid learning algorithm. For a useful tutorial reference one is referred to [13]. Based on its structure, one can construct a group of fuzzy rules, specifying the guidance commands with respect to three engagement phases. For briefness, only the guidance rules on the X-axis are presented. The guidance rules for the Y and Z axes can be derived analogously.

To form a standard ANFIS, the following the following Sugeno and Tsukamoto fuzzy models are first established.

(i) When $t_0 \le t \le t_A$,

R_j : IF κ_1 is A_1^j AND κ_2 is A_2^j AND κ_3 is A_3^j AND κ_4 is A_4^j,
THEN $\ddot{x}_c = k_1^j \dfrac{\kappa_1}{T_{go}} + k_2^j \dfrac{\kappa_2}{T_{go}} + k_3^j \dfrac{\kappa_3}{T_{go}} + k_4^j \dfrac{\kappa_4}{T_{goA}^2}$

(ii) When $t_A < t \le t_B$,

R_j : IF κ_1 is A_1^j AND κ_3 is A_3^j AND κ_5 is A_5^j,
THEN $\ddot{x}_c = k_5^j \dfrac{\kappa_1}{T_{go}} + k_6^j \dfrac{\kappa_3}{T_{go}} + k_7^j \dfrac{\kappa_5}{T_{goB}^2}$

(iii) When $t_B < t \le t_f$,

R_j : IF κ_1 is A_1^j AND κ_6 is A_6^j THEN $\ddot{x}_c = k_8^j \dfrac{\kappa_1}{T_{go}} + k_9^j \dfrac{\kappa_6}{T_{go}^2}$

where $\kappa_1 = \dot{x}_f - \dot{x}_0$ (velocity error), $\kappa_2 = \frac{\Delta x_2}{\Delta t_2} - \frac{\Delta x_1}{\Delta t_1}$ (curve change 1), $\kappa_3 = \frac{\Delta x_3}{\Delta t_3} - \frac{\Delta x_2}{\Delta t_2}$ (curve change 2), $\kappa_4 = x_1 - x_0 - \dot{x}_0 T_{goA}$ (position error at t_A), $\kappa_5 = x_2 - x_0 - \dot{x}_0 T_{goB}$ (position error at t_B) and $\kappa_6 = x_f - x_0 - \dot{x}_0 T_{go}$ (position error at t_f) with T_{go} being the time-to-go with respect to the interception point.

Then, to facilitate adaptation of the gain scheduling model, it is convenient to put the fuzzy model into the framework of an adaptive network. In the following, the output of the i-th node in the k-th layer is denoted by O_i^k.

Layer 1: Each node represents an input that passes an external signal to the next layer.
Phase 1: $O^1_{A_1^i} = \mu_{A_1^i}(\kappa_1)$, $O^1_{A_2^i} = \mu_{A_2^i}(\kappa_2)$, $O^1_{A_3^i} = \mu_{A_3^i}(\kappa_3)$, $O^1_{A_4^i} = \mu_{A_4^i}(\kappa_4)$, $i = 1, \ldots, m$
Phase 2: $O^1_{A_1^i} = \mu_{A_1^i}(\kappa_1)$, $O^1_{A_3^i} = \mu_{A_3^i}(\kappa_3)$, $O^1_{A_5^i} = \mu_{A_5^i}(\kappa_5)$, $i = 1, \ldots, m$
Phase 3: $O^1_{A_1^i} = \mu_{A_1^i}(\kappa_1)$, $O^1_{A_6^i} = \mu_{A_6^i}(\kappa_6)$, $i = 1, \ldots, m$
where m is the number of fuzzy sets with respect to the corresponding term-set of κ_i, the membership functions $\mu_{A_1^i}(\cdot)$, $\mu_{A_2^i}(\cdot)$, $\mu_{A_3^i}(\cdot)$ and $\mu_{A_{4,5,6}^i}(\cdot)$ are defined as follows

$$\mu_{A_1^i}(\kappa_1) = \exp\left\{ -\left(\frac{\kappa_1 - m_i}{\sigma_i} \right)^{b_i} \right\},$$

$$\mu_{A_2^i}(\kappa_2) = \exp\left\{ -\left(\frac{\kappa_2 - m_i}{\sigma_i} \right)^{b_i} \right\},$$

$$\mu_{A_3^i}(\kappa_3) = \exp\left\{ -\left(\frac{\kappa_3 - m_i}{\sigma_i} \right)^{b_i} \right\},$$

$$\mu_{A_l^i}(\kappa_l) = \exp\left\{ -\left(\frac{\kappa_l - m_i}{\sigma_i} \right)^{b_i} \right\}, \quad l = 4, 5, 6.$$

A desired membership function is obtainable by adjusting the parameter triplet (σ_i, b_i, m_i). Fig. 3 illustrates the initial bell-shaped membership functions.

Layer 2: Each node performs the product operation. Any t-norm operator can also be used as the node function for the generalized AND function.
Phase 1: ${}^jO^2 = \omega^j = \mu_{A_1^i}(\kappa_1)\mu_{A_2^i}(\kappa_2)\mu_{A_3^i}(\kappa_3)\mu_{A_4^i}(\kappa_4)$, $i = 1, \ldots, m$, $j = 1, \ldots, L\,(=m^4)$
Phase 2: ${}^jO^2 = \omega^j = \mu_{A_1^i}(\kappa_1)\mu_{A_3^i}(\kappa_3)\mu_{A_5^i}(\kappa_5)$, $i = 1, \ldots, m, j = 1, \ldots, L(=m^3)$
Phase 3: ${}^jO^2 = \omega^j = \mu_{A_1^i}(\kappa_1)\mu_{A_6^i}(\kappa_6)$, $i = 1, \ldots, m$, $j = 1, \ldots, L(=m^2)$.

Layer 3: Each node calculates the normalized firing strength of a rule.
Phase 1: ${}^jO^3 = \bar{\omega}^j = \frac{\mu_j}{\sum_j \mu_j}$, Phase 2: ${}^jO^3 = \bar{\omega}^j = \frac{\mu_j}{\sum_j \mu_j}$,
Phase 3: ${}^jO^3 = \bar{\omega}^j = \frac{\mu_j}{\sum_j \mu_j}$.

Layer 4: Each node calculates the weighted consequent value. The consequent parameters k_l^j, $l = 1, \ldots, 6$ are to be tuned.

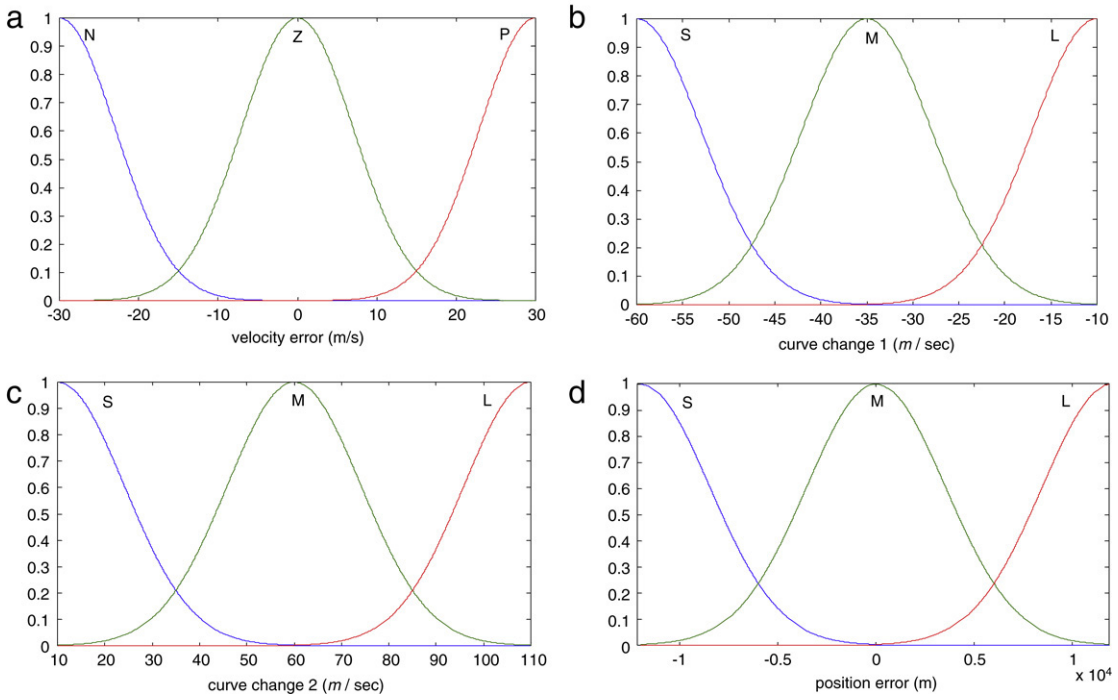

Fig. 3. Membership functions of the (a) velocity error (κ_1) (N: negative, Z: zero, P: positive); (b) curve change 1 (κ_2) (S: small, M: medium, L: large); (c) curve change 2 (κ_3); (d) position error ($\kappa_{4,5,6}$).

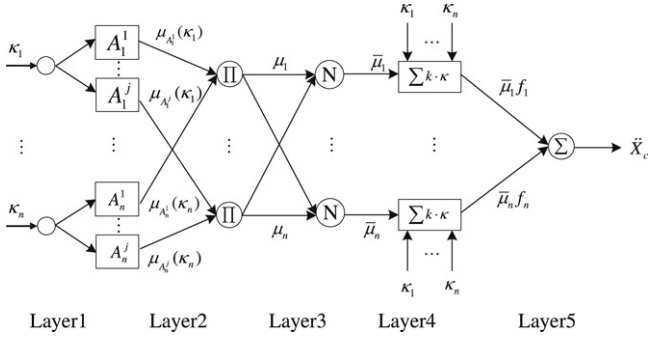

Fig. 4. Structure of the ANFIS.

Phase 1: ${}^jO^4 = \bar{\omega}^j f_j = \bar{\omega}^j (k_1^j \kappa_1 + k_2^j \kappa_2 + k_3^j \kappa_3 + k_4^j \kappa_4)$,
Phase 2: ${}^jO^4 = \bar{\omega}^j f_i = \bar{\omega}^j (k_1^j \kappa_1 + k_3^j \kappa_3 + k_5^j \kappa_5)$,
Phase 3: ${}^jO^4 = \bar{\omega}^j f_i = \bar{\omega}^j (k_1^j \kappa_1 + k_6^j \kappa_6)$.

Layer 5: Node i sums up all incoming signals to obtain the final inferred result.
Phase 1: $\ddot{x}_c = \sum_j \bar{\omega}^j f_j$, Phase 2: $\ddot{x}_c = \sum_j \bar{\omega}^j f_j$,
Phase 3: $\ddot{x}_c = \sum_j \bar{\omega}^j f_j$.

See Fig. 4 for the structure of the ANFIS. After an adaptive network which is functionally equivalent to a Sugeno and Tsukamoto fuzzy model has been constructed, the consequent parameters are regulated by a learning algorithm. This is presented as follows.

3.1. Adaptive guidance parameter update law

To aim at minimizing the kinetic energy loss, the following performance costs are defined:

Phase 1 : $E_1 = \frac{1}{2} \sum_{i=1}^{4} w_i \kappa_i^2$, $\sum_i w_i = 1$
Phase 2 : $E_2 = \frac{1}{2}(w_1 \kappa_1^2 + w_2 \kappa_3^2 + w_3 \kappa_5^2)$, $\sum_i w_i = 1$
Phase 3 : $E_3 = \frac{1}{2}(w_1 \kappa_1^2 + w_2 \kappa_6^2)$, $\sum_i w_i = 1$

where w_i, $i = 1 - 4$, are suitable weighting factors to fit the respective mission objective. For Phase 1, the conversion of kinetic energy to potential energy is significantly affected by the curvature change during $[t_0, t_2]$; therefore, it is heavily weighted. Similarly, for Phase 2, the curvature change during $[t_2, t_f]$ and the position error are jointly placed with larger weightings where the importance of position error emanates. For Phase 3, the position error is more important than the velocity error; therefore, set $w_2 > w_1$.

Adaptive tuning equations for k_l^j, m_l^j, and σ_l^j are summarized as follows.

Phase 1: k_l^j, m_l^j, σ_l^j $(b_i^j = 1)$, $l = 1 - 4, j = 1, \ldots, L$

$$k_l^j(t+1) = k_l^j(t) + \Delta k_l^j(t)$$

where

$$\Delta k_l^j(t) = -\eta \nabla_{k_l^j} E_1(t) = \eta \left[-w_1 \kappa_1 \frac{\partial x_0}{\partial \ddot{x}_c} + w_2 \kappa_2 \frac{\partial (x_0/\Delta t_1)}{\partial \ddot{x}_c} + w_3 \kappa_3 \frac{\partial (x_f/\Delta t_3)}{\partial \ddot{x}_c} - w_4 \kappa_4 \frac{\partial (x_0 + \dot{x}_0 T_{goA})}{\partial \ddot{x}_c} \right] \frac{\partial \ddot{x}_c}{\partial k_l^j}$$

with η, $1 \gg \eta > 0$, being the update gain and $\frac{\partial \ddot{x}_c}{\partial k_l^j} = \frac{\mu_j}{\sum_j \mu_j} \kappa_l$.

Similarly, the parameter update equations for m_i^j are determined via

$$m_l^j(t+1) = m_l^j(t) + \Delta m_l^j(t)$$

where

$$\Delta m_l^j(t) = -\eta \nabla_{m_l^j} E_1(t) = \eta \left[-w_1 \kappa_1 \frac{\partial x_0}{\partial \ddot{x}_c} + w_2 \kappa_2 \frac{\partial (x_0/\Delta t_1)}{\partial \ddot{x}_c} + w_3 \kappa_3 \frac{\partial (x_f/\Delta t_3)}{\partial \ddot{x}_c} \right.$$

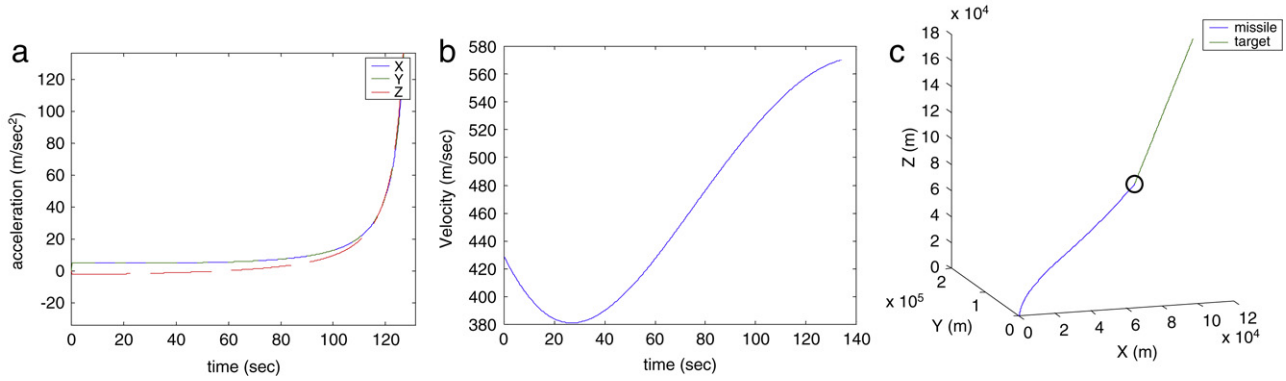

Fig. 5. (a) Inertia control command, (b) missile velocity, (c) engagement trajectory.

$$- \; w_4\kappa_4 \frac{\partial(x_0 + \dot{x}_0 T_{goA})}{\partial \ddot{x}_c} \Bigg] \frac{\partial \ddot{x}_c}{\partial m_l^j}$$

with

$$\frac{\partial \ddot{X}_c}{\partial m_l^j} = \frac{\partial \ddot{X}_c}{\partial y} \frac{\partial y}{\partial \mu_j} \frac{\partial \mu_j}{\partial \mu_{A_l^j}} \frac{\partial \mu_{A_l^j}}{\partial m_l^j} = \frac{\mu_j}{\sum_j \mu_j} \frac{\partial y}{\partial \mu_j} \mu_j \frac{2(\kappa_l - m_l^j)}{{\sigma_l^j}^2}.$$

And

$$\sigma_l^j(t+1) = \sigma_l^j(t) + \Delta\sigma_l^j(t)$$

where

$$\begin{aligned} \Delta\sigma_l^j(t) &= -\eta \nabla_{\sigma_l^j} E_1(t) \\ &= \eta \Bigg[-w_1\kappa_1 \frac{\partial x_0}{\partial \ddot{x}_c} + w_2\kappa_2 \frac{\partial(x_0/\Delta t_1)}{\partial \ddot{x}_c} + w_3\kappa_3 \frac{\partial(x_f/\Delta t_3)}{\partial \ddot{x}_c} \\ &\quad - \; w_4\kappa_4 \frac{\partial(x_0 + \dot{x}_0 T_{goA})}{\partial \ddot{x}_c} \Bigg] \frac{\partial \ddot{x}_c}{\partial \sigma_l^j} \end{aligned}$$

with

$$\frac{\partial \ddot{X}_c}{\partial \sigma_l^j} = \frac{\partial \ddot{X}_c}{\partial y} \frac{\partial y}{\partial \mu_j} \frac{\partial \mu_j}{\partial \mu_{A_l^j}} \frac{\partial \mu_{A_l^j}}{\partial \sigma_l^j} = \frac{\mu_j}{\sum_j \mu_j} \frac{\partial y}{\partial \mu_j} \mu_j \frac{2(\kappa_l - \sigma_l^j)^2}{{\sigma_l^j}^3}.$$

Phase 2: $k_l^j, m_l^j, \sigma_l^j (b_l^j = 1), l = 1, 3, 5, j = 1, \ldots, L$

$$\begin{aligned} k_l^j(t+1) &= -\eta \nabla_{k_l^j} E_2(t) \\ &= k_l^j(t) + \eta \Bigg[-w_1\kappa_1 \frac{\partial x_0}{\partial \ddot{x}_c} + w_2\kappa_3 \frac{\partial(x_f/\Delta t_3)}{\partial \ddot{x}_c} \\ &\quad - \; w_3\kappa_5 \frac{\partial(x_0 + \dot{x}_0 T_{goB})}{\partial \ddot{x}_c} \Bigg] \frac{\partial \ddot{x}_c}{\partial k_l^j} \end{aligned}$$

$$\begin{aligned} m_l^j(t+1) &= m_l^j(t) + \eta \Bigg[-w_1\kappa_1 \frac{\partial x_0}{\partial \ddot{x}_c} + w_2\kappa_3 \frac{\partial(x_f/\Delta t_3)}{\partial \ddot{x}_c} \\ &\quad - \; w_3\kappa_5 \frac{\partial(x_0 + \dot{x}_0 T_{goB})}{\partial \ddot{x}_c} \Bigg] \frac{\partial \ddot{x}_c}{\partial m_l^j} \end{aligned}$$

$$\begin{aligned} \sigma_l^j(t+1) &= \sigma_l^j(t) + \eta \Bigg[-w_1\kappa_1 \frac{\partial x_0}{\partial \ddot{x}_c} + w_2\kappa_3 \frac{\partial(x_f/\Delta t_3)}{\partial \ddot{x}_c} \\ &\quad - \; w_3\kappa_5 \frac{\partial(x_0 + \dot{x}_0 T_{goB})}{\partial \ddot{x}_c} \Bigg] \frac{\partial \ddot{x}_c}{\partial \sigma_l^j}. \end{aligned}$$

Phase 3: $k_l^j, m_l^j, \sigma_l^j (b_l^j = 1), l = 1, 6, j = 1, \ldots, L$

$$\begin{aligned} k_l^j(t+1) &= -\eta \nabla_{k_l^j} E_3(t) \\ &= k_l^j(t) + \eta \Bigg[-w_1\kappa_1 \frac{\partial x_0}{\partial \ddot{x}_c} + w_2\kappa_6 \frac{\partial \kappa_6}{\partial \ddot{x}_c} \Bigg] \frac{\partial \ddot{x}_c}{\partial k_l^j} \end{aligned}$$

$$m_l^j(t+1) = m_l^j(t) + \eta \Bigg[-w_1\kappa_1 \frac{\partial x_0}{\partial \ddot{x}_c} + w_2\kappa_6 \frac{\partial \kappa_6}{\partial \ddot{x}_c} \Bigg] \frac{\partial \ddot{x}_c}{\partial m_l^j}$$

$$\sigma_l^j(t+1) = \sigma_l^j(t) + \eta \Bigg[-w_1\kappa_1 \frac{\partial x_0}{\partial \ddot{x}_c} + w_2\kappa_6 \frac{\partial \kappa_6}{\partial \ddot{x}_c} \Bigg] \frac{\partial \ddot{x}_c}{\partial \sigma_l^j}.$$

The lateral acceleration commands obtained above have to be transformed to the interceptor's body frame by applying the following coordinate transformation:

$$\begin{bmatrix} a_{my} \\ a_{mp} \end{bmatrix}_{\text{body}} = [\ell] \begin{bmatrix} \ddot{x}_c \\ \ddot{y}_c \\ \ddot{z}_c \end{bmatrix}$$

where a_{my} and a_{mp} indicate, respectively, the lateral acceleration commands on the horizontal and vertical planes, and the coordinate transformation matrix ℓ is defined as

$$[\ell] = \begin{bmatrix} \sin\phi \sin\gamma \cos\psi - \cos\phi \sin\psi & \sin\phi \sin\gamma \sin\psi + \cos\phi \cos\psi & \sin\phi \cos\gamma \\ \cos\phi \sin\gamma \cos\psi + \sin\phi \sin\psi & \cos\phi \sin\gamma \sin\psi - \sin\phi \cos\psi & \cos\phi \cos\gamma \end{bmatrix}$$

where ϕ, ψ, γ are, respectively, the roll angle, the azimuth angle, and the flight-path angle.

4. Results and analyses

First, a target with the incoming speed of 212 m/s and flight path angle of 70.5 degrees was considered. In this case, the initial target position was (60000, 60000, 140000) (m). Fig. 5 shows the control history, velocity, and engagement trajectory with the interceptor simply guided by the adaptive S-2 guidance law. The total flight time is 132.1 s. Fig. 6 shows the results for the same scenario, along with the interceptor guided by S-2 guidance law with constant gains. The total flight time is 197 s, which is much longer than the previous adaptive case.

For the second scenario, we considered the initial target position at (60000, 60000, 140000) (m). The two via points of interceptor's flight trajectory were set at (10000, 10000, 6000) (m) and (20000, 20000, 5000) (m). The interceptor was guided by the adaptive S-4 guidance law. Fig. 7 shows the control history, missile velocity, and engagement trajectory. Estimations of T_{go}, T_{goA}, and T_{goB} are displayed in Fig. 8. The resulting trajectory shows a successful target engagement with the proposed guidance design.

To verify robustness of the engagement performance, we have considered the setting with the initial target position at (60000, 60000, 30000) (m), midpoint A at (10000, 10000, 6000) (m), and midpoint B at (20000, 20000, 6000) (m). Fig. 9 shows the control history, missile velocity, and engagement trajectory. Although midpoint B was intentionally placed at an unfavorable position, the guidance law can still steer the interceptor to an interception point.

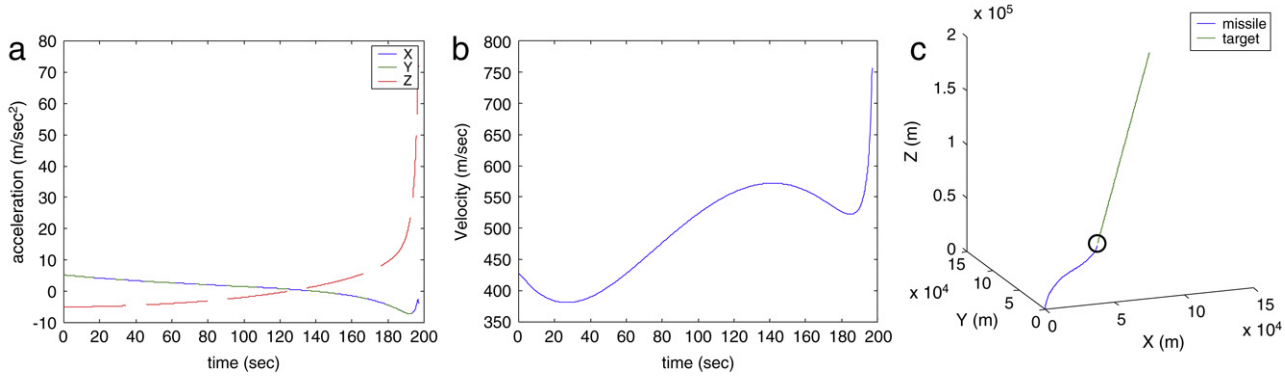

Fig. 6. (a) Inertia control command, (b) missile velocity, (c) engagement trajectory.

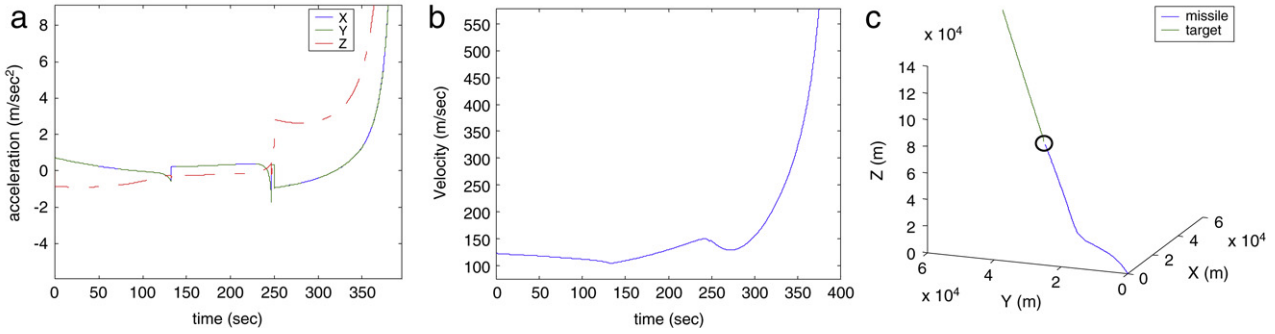

Fig. 7. (a) Inertia control command, (b) missile velocity, (c) engagement trajectory.

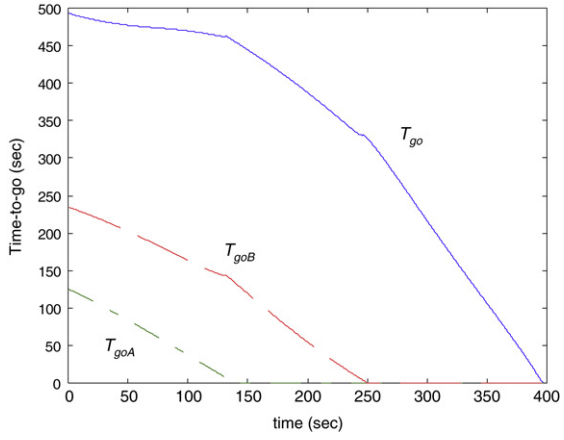

Fig. 8. Estimation of time-to-go.

Fig. 10(a) plots the comparison of S-4 guidance law with constant and adaptive gains. Fig. 10(b) illustrates two interceptor flight trajectories with the midpoint A set to be (10000, 10000, 6000) (m) and (100000, 100000, 8000) (m), respectively. Ultimately, the performance robustness of the adaptive S-4 guidance law to variations of the midpoints at the desired flight trajectory is thus verified.

5. Conclusion

This paper proposes an adaptive trajectory shaping guidance scheme which introduces a fuzzy system model to represent gain scheduling variables and realize a generalized spline guidance law. The spline guidance law is developed with the aim of shaping the interceptor's flight trajectories for the missile's energy conservation and performance robustness. It is shown that the proposed guidance law yields excellent interception performance against a variety of targets. It is believed that the generalized guidance scheme could be served as a basis for the development

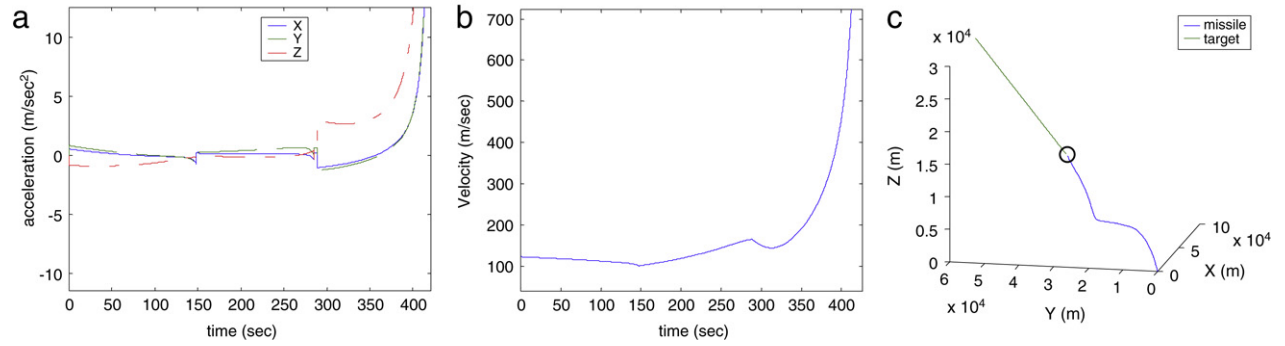

Fig. 9. (a) Inertia control command, (b) missile velocity, (c) engagement trajectory.

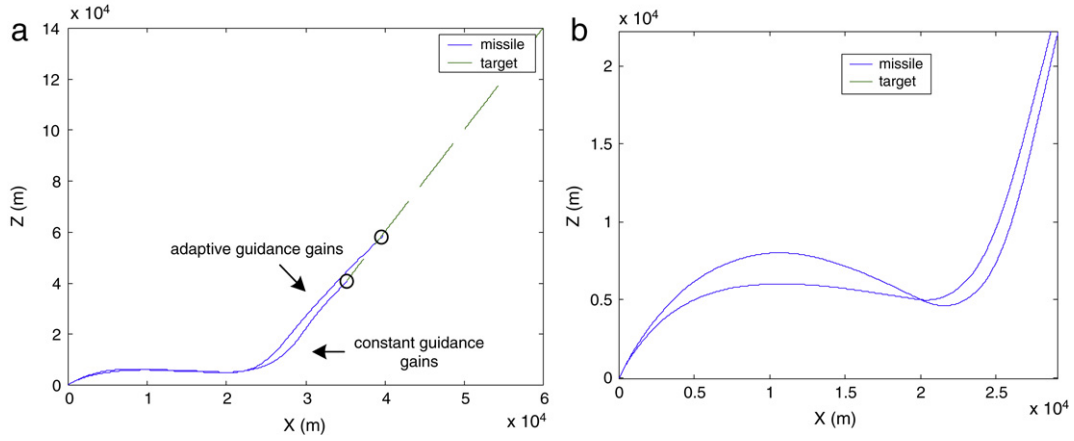

Fig. 10. (a) Comparison of S-4 guidance law with constant gains and adaptive gains, (b) trajectories generated by different midpoints.

of a wide variety of mission oriented guidance laws, such as cruise missile guidance, anti-ballistic missile guidance, etc.

Acknowledgements

This research was sponsored in part by the Ministry of Education, Taiwan, ROC under the ATU plan.

References

[1] Hardtla JW, Milligan KH, Cramer EJ. Design and implementation of a missile guidance law derived from modern control theory. AIAA Paper 87-2447; 1987.
[2] Newman B. Strategic intercept midcourse guidance using modified zero effort miss steering. AIAA Journal of Guidance and Control 1996;9:107–12.
[3] Bezick S, Gray WS. Guidance of a homing missile via nonlinear geometric control methods. AIAA Journal of Guidance, Control, and Dynamics 1995;18: 441–8.
[4] Song EJ, Tahk MJ. Three-dimensional midcourse guidance using neural networks for interception of ballistic targets. IEEE Transactions on Aerospace and Electronic Systems 2002;38:19–24.
[5] Jang JSR. ANFIS: Adaptive-network-based fuzzy inference system. IEEE Transactions on Systems, Man, Cybernetics 1993;23:665–85.
[6] Mishra K, Sarma IG, Swamy KN. Performance evaluation of two fuzzy-logic-based homing guidance schemes. AIAA Journal of Guidance, Control, and Dynamics 1994;17:1389–91.
[7] Lin CM, Mon YJ. Fuzzy-logic-based guidance law design for missile systems. In: Proceedings of IEEE international conference on control applications. 1999. p. 421–426.
[8] Lin CL, Su HW. Adaptive fuzzy gain scheduling in guidance system design. AIAA Journal of Guidance, Control, and Dynamics 2001;24:683–92.
[9] Elhalwagy YZ, Tarbouchi M. Fuzzy logic sliding mode control for command guidance law design. ISA Transactions 2004;43:231–42.
[10] Cherry GW. A general explicit, optimizing guidance law for rocket-propellant spacecraft. AIAA Paper 64-638; 1964.
[11] Burden RL, Faires JD, Reynolds AC. Numerical analysis. Brooks/Cole; 1997.
[12] Press WH, Flannery BP, Teukolsky SA, Vetterling WT. Numerical recipes in FORTRAN: The art of scientific computing. Cambridge University Press; 1992.
[13] Jang JSR, Sun CT, Mizutani E. Neuro-fuzzy and soft computing. Prentice-Hall Inc.; 1997.